

PAPER • OPEN ACCESS

Effect of Microstructures in Microchannel for Single Phase Flow Mixing Intensification

To cite this article: Fiona W M Ling *et al* 2020 *IOP Conf. Ser.: Mater. Sci. Eng.* **736** 022032

View the [article online](#) for updates and enhancements.



The Electrochemical Society
Advancing solid state & electrochemical science & technology

240th ECS Meeting ORLANDO, FL

Orange County Convention Center Oct 10-14, 2021



Abstract submission due: April 9

SUBMIT NOW

Effect of Microstructures in Microchannel for Single Phase Flow Mixing Intensification

Fiona W M Ling^{1,2}, Ali A. Khleif³ and Hayder A Abdulbari^{1,2*}

¹ Centre of Excellence for Advanced Research in Fluid Flow (CARIFF), Universiti Malaysia Pahang, 26300 Gambang, Pahang, Malaysia.

² Faculty of Chemical & Natural Resources Engineering, Universiti Malaysia Pahang, 26300 Gambang, Pahang, Malaysia.

³ Department of Production Engineering and Metallurgy, University of Technology-IRAQ, Baghdad, IRAQ

*Corresponding author: hayder.bari@gmail.com

Abstract. Enhancing flow in microchannel is a serious fundamental challenge due to the laminar flow nature of the liquids in the microscale systems that prevents the traditional viscoelastic additives from interacting with the turbulence structures (eddies) for an effective drag reduction performance. Passive drag reduction technique is believed to be a promising solution and never been investigated in the microflow systems before. In this work, micro-riblets (V-shaped) with the size ranging from 20 to 100 μm were designed, fabricated, and placed at the narrow side-walls of the rectangular microchannel in an attempt to test its flow enhancement performances. The microchannels were fabricated through a direct writing method where polymethylsiloxane was used as the substrate. The flow behavior was investigated through monitoring the flow rate of the fluids flowing through the system. The flow profile in the system was evaluated using micro-particle velocimetry (μ -PIV). The results indicated a flow enhancement up to $\sim 29\%$ for a 60 μm of base-to-height riblet at an operating pressure of ~ 200 mbar for a single phase flow system. Larger micro-riblets were found to produce a thicker laminar sublayer within the devices that narrowed the active core of the solution.

1. Introduction

Passive drag reduction techniques for enhancing flow in pipes and conduits has attracted the attention of many researchers in the past few decades due to its economic and academic potentials [1–3]. The microstructures observed over the shark skin, which is believed to be one of the factors that boosts the shark speed in water, has inspired many researchers like Bechert, Bruse, Hage, Vav Der Hoeven and Hoppe [4], Bixler and Bhushan [5], and B. Dean and Bhushan [6] to simulate these structures in the attempts to enhance the flow of submerged surfaces [7–9]. Unfortunately, most of the experimentally investigated structures did not show high drag reduction effect when compared with the active techniques that utilize viscoelastic additives for drag reduction like polymers [10–14], surfactants [15,16], or even suspended solids [17,18]. Fu, Yuan and Bai [19] investigated the effect of five different riblets geometries (V, L, U, \cap , and space-V) on drag reduction (DR) performance using FLUENT. The authors reported that the \cap -shaped riblets increased the drag yet other geometries



demonstrated DR in the order of 1%–5%. From the study, the L geometry surface possessed the highest DR performance but the surface faced difficulties in fabrication. Thus, the V-shaped riblets are more practical and at the same time have good DR efficiency. Chen and coworkers proposed and investigated the impact of the biomimetic herringbone riblets which is similar to birds' feather structure on DR operation [20]. The authors reported that a remarkable DR of up to 16% was observed when the water flowed through the structures. The phenomena was due to the maximum shear stress concentrated at the tips of the riblets structures and the thickening of the viscous sublayer. Kim et al. [21] reported that 20% of DR was observed when water flowed through the channel with micro-riblets and the efficiency increased up to 36% when utilizing a hierarchically engineered surface that had both micro-riblets and nanostructures. Also, it is believed that this technique could be effective over a large flow regime range [22].

It is believed that longitudinal riblets can result in a lower shear stress in flow than that of a smooth surface [23,24]. The structures act as small fences that restrict span-wise movement of vortices thus reducing and limiting the occurrence of bursts. These bursts contribute to most of the shear stresses within the system. During the bursts, low speed fluids move from near-wall region toward the high velocity bulk fluid in the center leading to the splatter of high speed liquid against the wall [25]. Therefore, a grooved surface prevents random low-speed streaks from converging into an ejection thus reducing the pressure drop. The riblet protrusion height is an important parameter that is the offset between the virtual origin of a stream-wise shear flow and some mean surface locations. Compared with a smooth wall, this offset results in a greater separation between the wall and the turbulent stream-wise vortices, reducing the momentum exchange at the wall [26,27]. Therefore, it is clear that the DR effect and the function of the micro-riblets is highly influenced by the dimensions of the carrying conduit (pipe or channel) where the liquid rheological properties domination controls the flow pattern.

The flow of liquids in microchannels is dominated by many physical properties that have less effect in larger size structures (pipes and conduits) where all the flow is laminar and no clear turbulence is observed in most cases [28–30]. Such fact introduces a new challenge to the researchers in the active DR field where the interaction between the additives and turbulence structures (eddies) is essential for a good flow enhancement effect [31–33]. On the other hand, structuring the wide base of rectangular microchannel helps in enhancing the mixing performance in micromixers through chaotic advection methods that will change the flow pattern along the microchannel [34–36]. The chaotic regime in the system can disperse the fluids effectively by creating eddy-based flow patterns in regular flow fields [37–40] and stretches or folds fluid volumes [41,42]. It is important to note that stretching increases the length of the interface while folding constrains the fluid to fill a finite region [43]. When the length of the fluid boundary grows exponentially with time due to the stretching–folding mechanism, the diffusion will enhance and this results in a higher mixing performance [44]. Wu, Hsu and Feng [45] observed a complete mixing in 0.08 s when cylindrical obstacles were embedded within their micromixer system. Cortes-Quiroz, Azarbadegan, Zangeneh and Goto [46] reported a high mixing index of up to 0.83 through a grooved micromixer with a staggered herringbone structure, and that the mixing performance increased with the groove width.

It is believed that the presence of micro-riblets on the narrow side walls of the rectangular microchannel can have a positive effect on the flow enhancement. In the present work, we are aiming to evaluate the flow enhancement effect of V-shaped riblets on the side walls of microchannels with different dimensions. The experiments were conducted using an open-loop liquid flow system and the flow enhancement performances were evaluated using flow rate measurements at different water flow rates. The flow patterns were observed using micro-particle velocimetry (μ -PIV) technique.

2. Experimental Details

2.1. Materials

In this work, SU-8 photoresist (GM1070 for layers between 15-200 μm) and SU-8 developer were purchased from Gersteltec and used without further purification. Sylgard 184 silicone elastomer kit

which consisted of Polydimethylsiloxane (PDMS) and its curing agents were purchased from Dow Corning and was used as the substrate of micromixer.

2.2. Micromixers design and fabrication

Five T-shaped micromixers with V-shaped microriblets located along the narrow side (channel wall) were first designed using AutoCAD software. The dimensions of the structures were varied in base and height where the ratio of the base to the height was 1:1, as shown in Figure 1 and Table 1. The micromixers were fabricated by adopting a direct writing method as shown in **Error! Reference source not found.** A new clean 4-inch silicon wafer was placed at the centre of the spin coater (model: Laurell WS-650-23B, USA) chuck. 5.5 ml of SU-8 photoresist were pipetted using a micropipette and photoresist were delivered on the centre of the wafer. To obtain 100 μm thickness of SU-8 on the wafer, the spin coater was set according to the following steps: 500 rpm at the acceleration of 100 rpm/s for 10 s then increased to 900 rpm for 30 s with the acceleration of 300 rpm/s. The wafer was put on a flat surface for relaxing step for overnight before proceeding the next procedure. Then, the wafer was brought for soft baking process at 65 °C for 15 min then at 95 °C for 40 min with the ramping 2 °C/min. When the wafer had cool down to room temperature, it was loaded in a micro-pattern generator (μPG) to expose the design on the wafer. After exposure, the wafer was brought for post baking at 65 °C for 15 min then at 95 °C for 40 min. After the wafer was cooled to room temperature, the wafer was soaked in 80 ml of SU-8 developer for 5 min and agitated softly to remove the unexposed SU-8. The developed wafer was then baked at 135 °C for 2 h.

In this work, PDMS was the substrate of the micromixer. PDMS and its curing agent was first weighed in a disposable plastic cup with a ratio of 10:1 by weight where in this work 60 g and 6 g of PDMS and curing agent were used, respectively. The mixture was then mixed vigorously for 5 min at 1000 rpm using a planetary centrifugal mixer (Thinky, USA) and degassed at 400 rpm for another 5 min. The wafer was cleaned using nitrogen gun and placed in a clean petri dish before the PDMS mixture was poured on the wafer. The petri dish was put in a desiccator for at least 40 min to remove all the trapped air bubbles. Then, the PDMS was baked in an oven at 80 °C for 2 h. PDMS was cut along the edge of the wafer using a scalpel and peeled off carefully from the wafer using a tweezer. The inlet and outlet of the microchannel were punched using a puncher. Both of PDMS and a new clean glass slide were placed in a plasma cleaner (Harrick Plasma, USA) for 2 min with the design of the microchannel facing upward. Both surfaces were then put together with the design of microchannel facing the glass slide and pressed slightly to let them adhere together.

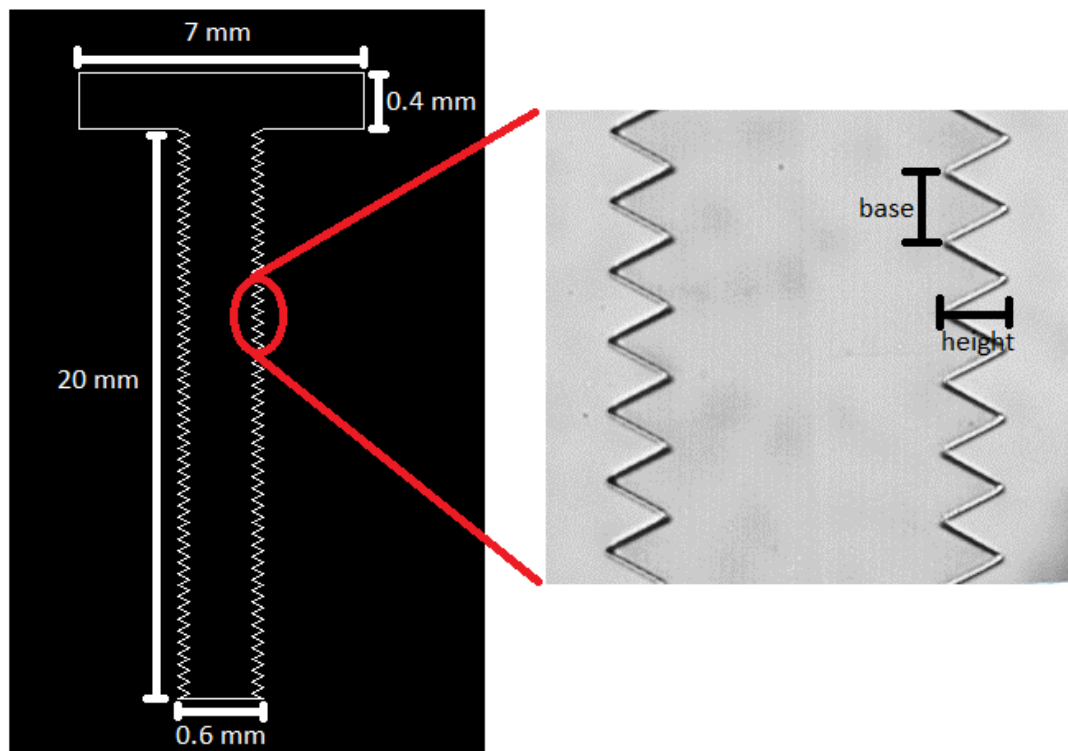


Figure 1. Overall dimension of designed microchannel with microriblets profile

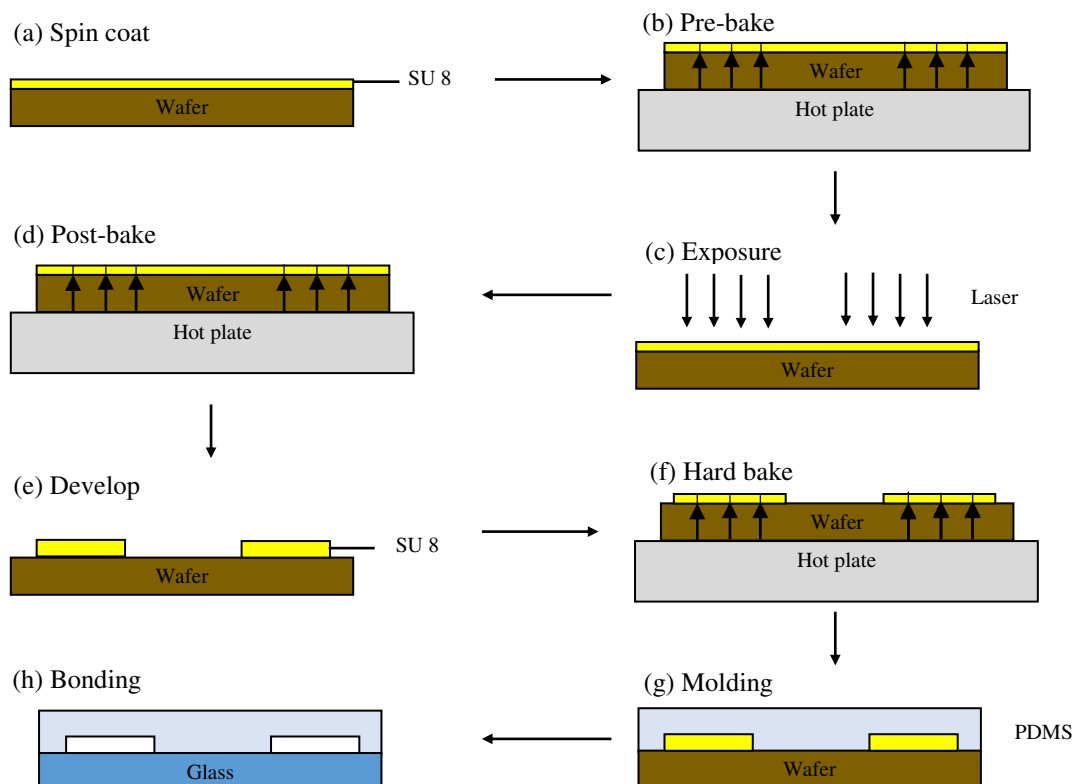
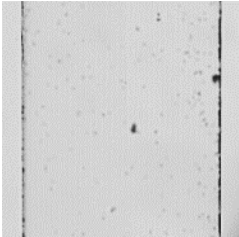
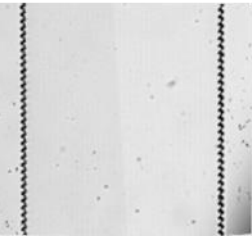
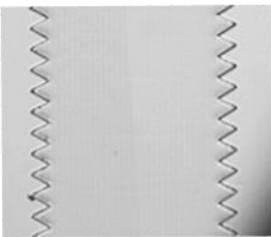
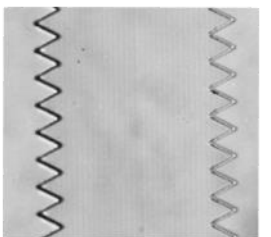
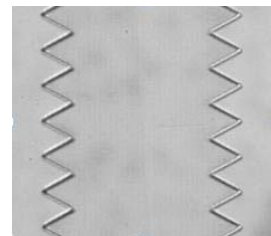
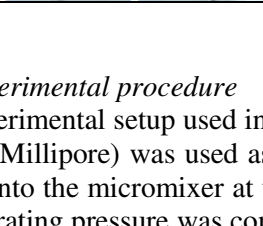


Figure 2. Schematic diagram of direct writing fabrication method

Table 1. Dimensions of microriblets

Model		Total length of inlet channels	Total length of mixing channel	Width of inlet channel	Width of mixing channel
		7 mm	20 mm	0.4 mm	0.6 mm
		Microriblets Dimension (μm)			
		Height		Base	
1		0		0	
2		20		20	
3		60		60	
4		80		80	
5		100		100	

2.3. Experimental procedure

The experimental setup used in this work was previously reported by us in [13,14,47]. Ultrapure water (model: Millipore) was used as the working fluid for the whole experiment. The ultrapure water was flowed into the micromixer at the operating pressure of 200 – 900 mbar with an interval of 100 mbar. The operating pressure was controlled using the Elveflow Smart Interface by executing the commands to the pressure and vacuum controller to push the water out from the reservoir. The flow rate across

the tube length was measured and recorded responding to the operating pressure. The steps were repeated for all the micromixers with different microriblets size.

The flow enhancement performance was evaluated using the equation as below:

$$\%FI = \frac{F_a - F_b}{F_a} \times 100 \quad (1)$$

where,

%FI = percentage of flow rate increment

F_a = flow rate of ultrapure water in control micromixer (no microriblet)

F_b = flow rate of ultrapure water in micromixers with microriblet

μ -PIV was used to obtain the flow profile within the micromixers as reported previously by Abdulbari and Ling [13]. The main interest areas of the micromixer in this work were the mixing point where both inlets met (region 1) and the straight channel (region 2 and 3) as shown in Figure 3. The fluid containing ultrapure water and 8- μ m diameter Rhodamine B fluorescent particle (MicroVec MV-F07) was prepared. To obtain accurate instantaneous velocity fields, the volumetric particle concentration was prepared at 0.07%. The fluid was immersed in ultrasonic bath for 2 minutes to prevent the agglomeration of the particles. The micromixer was placed on the microscope stage and adjustment was done to have clear image of the interest area. The same setting as in [13,14,47] was used to control the flow of the Rhodamine B fluorescent particles solution. A double-pulsed Nd:YAG laser with 200 mJ pulse energy was focused on the object plane by a microscope (Nikon ECLIPSE Ni-U). The 532-nm incident laser light was expanded and reflected by an epifluorescent filter (dichroic mirror) before illuminating particles within a volume of fluid through an objective lens. The fluorescence excitation and particle-scattered light followed the same path through the microscope objective and the dichroic mirror. Excitation and emission peak wavelengths of 532 and 590 nm, respectively, were recorded where the fluorescent particles absorbed green incident light and emitted red light. The images with the time interval of 8 μ s were recorded using a 5 MP CCD camera (IMPERX CLB-B2520M-SC) with a 2456 \times 2058 pixel array. Instantaneous velocity vectors were derived from a two-frame cross-correlation, and 46 pairs of frames were averaged to obtain the mean velocity profiles. The interrogation window was set to 64 \times 32 pixels (streamwise \times spanwise direction) and 50% overlap. The results were then interpreted using Tecplot 360 software. Both the inlets were ultrapure water and was mixed with the fluorescent particle.

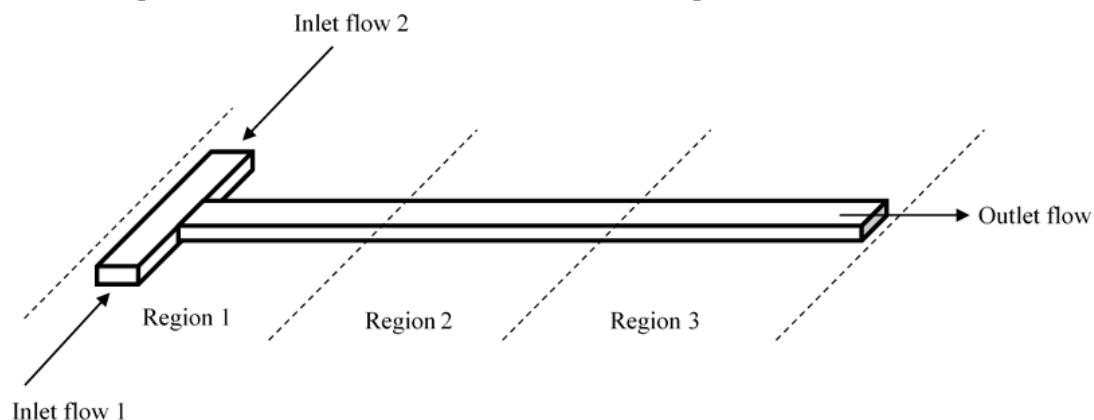


Figure 3. Main interest of analysis location in the micromixer

3. Results and Discussions

3.1. Flow enhancement

Figure 4 shows the flow enhancement performance of the micromixers with different riblets dimensions. From the results, it can be seen that the %FI was in positive region for low operating

pressure of 200 mbar indicating the microstructures reduced the skin friction of the fluid flow resulting in an increase of fluid velocity within the system. The flow enhancement performance achieved the highest %FI of 28.73% when increasing the microriblets size from 20 to 60 μm . However, continuous increasing the microriblets size showed negative effect where the %FI reduced slightly to 25.95% and 20.65% for the microriblets size of 80 and 100 μm , respectively. Similar pattern was also observed for higher operating pressure (300–900 mbar). It is believed that the presence of microriblets will create a stagnant liquid layer that replaces the solid surface in the case of smooth surface. The stagnant liquid layer depth trapped in the V-shaped valleys will depend on the dimensions of the grooves and its mobility will be affected as well with the surface tension–water mass relationship that gets weaker when the groove is deeper. It is expected that increasing the space between the microriblets leads to the formation of some secondary vortices that enter the gaps and increase the shear stress [6]. Hence, the flow enhancement performance was lower when utilizing larger microriblets. The results also agreed with the literature where the optimum micro-riblets spacing was 30–70 μm [26,48,49]. In this study, a maximum %FI of 28.73% was achieved from a microchannel with the 60 μm microriblets at the operating pressure of 200 mbar.

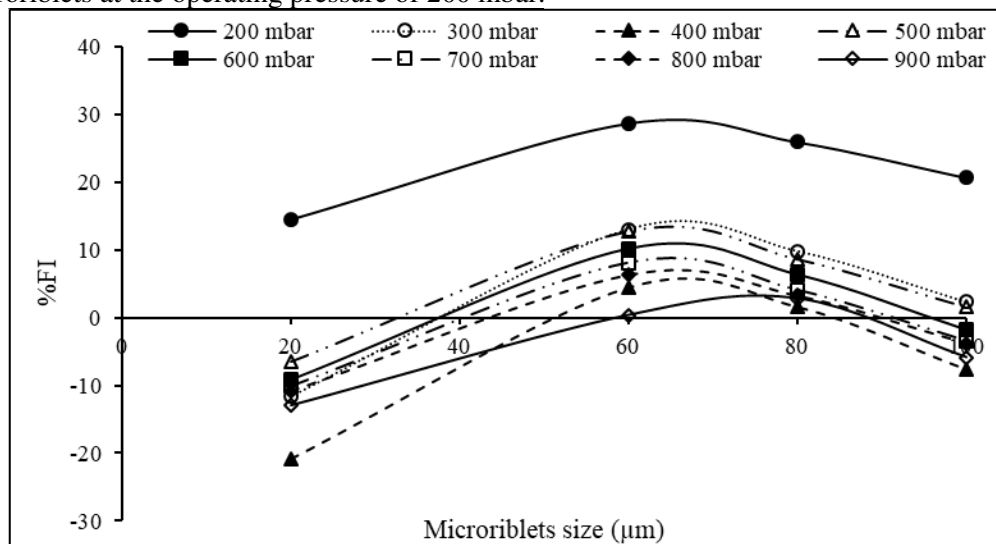


Figure 4. %FI of different microchannel with different microriblets size at operating pressure ranging from 200 to 900 mbar

3.2. Mixing profile

The flow profile within the micromixers were obtained by conducting μ -PIV measurements. Figure 5–Figure 10 demonstrate the velocity profile for single phase system (ultrapure water as working fluid) at different test sections as described before in Figure 3. In Region 1, the liquid velocity was 0.38 m/s for the smooth wall channel (Figure 5a) and decreased slightly to 0.36 m/s for 20 μm ribletted channel (Figure 5b). However, within the microchannels with 60 μm microriblets, the liquid velocity increased about 32% reaching 0.5 m/s. The liquid velocities decreased to 0.44 and 0.26 m/s when increasing the microriblets dimension to 80 and 100 μm . The results agreed with the flow enhancement experimental results discussed in Section 3.1 (Figure 4) where 60 μm ribletted channel achieved the highest %FI and larger micro-riblets size had a negative effect on the flow enhancement.

In Region 2, the water velocity of the smooth wall channel was around 0.34 m/s and increased slightly to 0.37 m/s in 20 μm ribletted channel as shown in Figure 6a and b. Continue increases the riblets size however decreases the average liquid velocity as illustrated in Figure 6d–f. High velocity regions can be observed at the near wall within the smooth wall channel and also small (20 and 60 μm) ribletted channels. With larger microriblets size, high velocity pockets were observed at the active core of the system. The large microriblets thickened the liquid sublayer thus compressed the flow in the middle of the channel resulting in narrow active core within the micromixer (Figure 6). Similar

flow behavior was observed in Region 3 (Figure 7) of the microchannels where the velocity decreased within the larger microriblets and thicker sublayer was formed in the system.

By increasing the operating pressure from 200 to 300 mbar, the average velocity of the liquid increased at least 50% up to the maximum velocity of more than 0.7 m/s in all the microchannels as demonstrated in the Figure 8–Figure 10. Similar flow behaviour was also observed at higher operating pressure where increasing the microriblets size increased the average velocity within the investigated region. Beyond riblets size of 60 μm , it showed negative effect on the flow enhancement performance. The liquid velocity dropped about 30% to 0.35 m/s within the 60 μm ribleted channel as shown in Figure 9c. Increasing the riblets size along the channel wall did not have significant effect in flow enhancement where the average velocity was about the same as in 60 μm -microriblets system. In Regions 2 (Figure 9) and 3 (Figure 10) the flow velocities were lower than that within the smooth wall microchannels. A thicker laminar sublayer was also observed within the microchannels with larger microriblets size (60–100 μm).

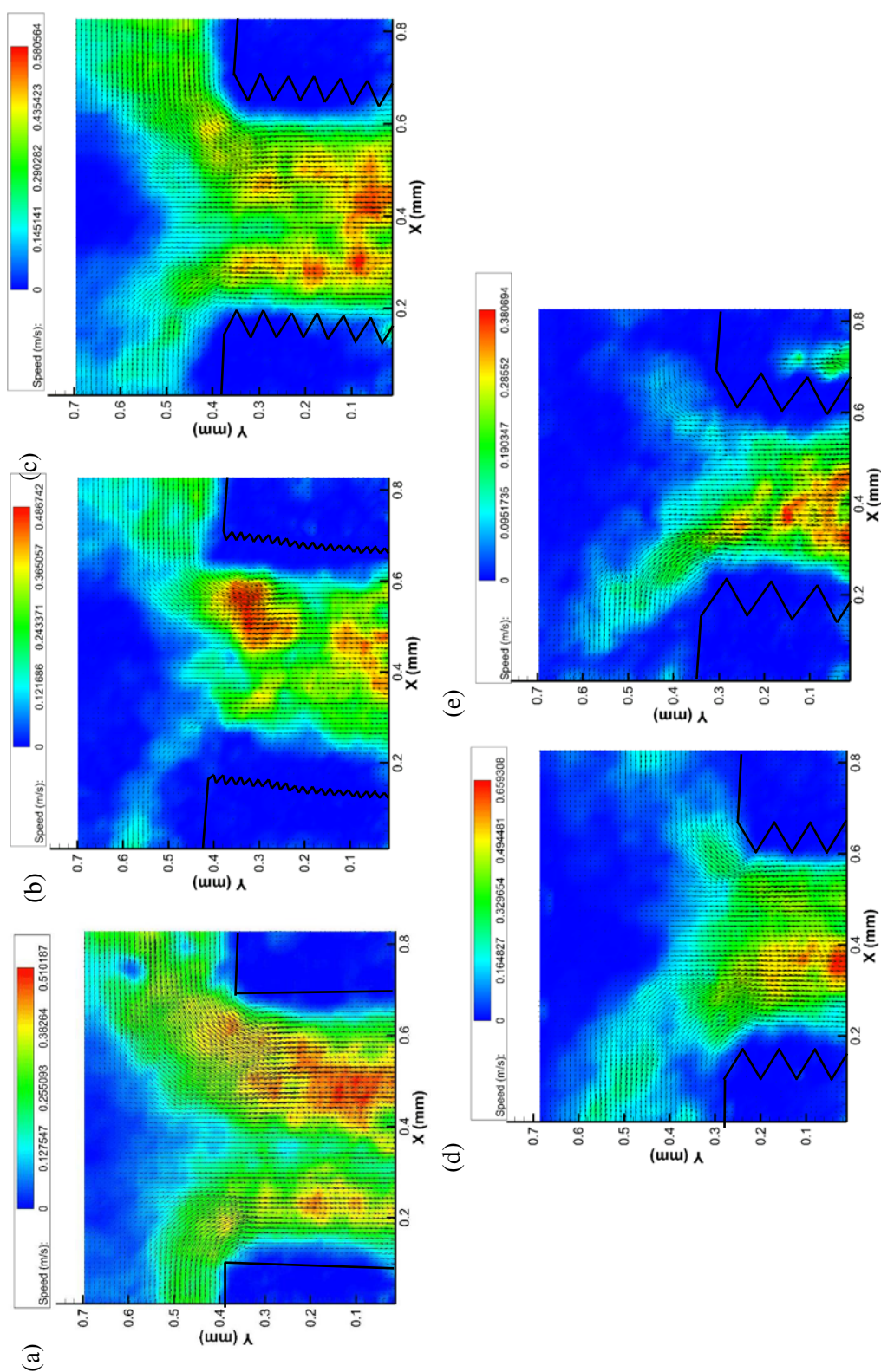


Figure 5. Velocity profile of microchannels (a) without microriblets, with microriblets size of (b) 20 μm , (c) 60 μm , (d) 80 μm , and (e) 100 μm at region 1 with the operating pressure of 200 mbar

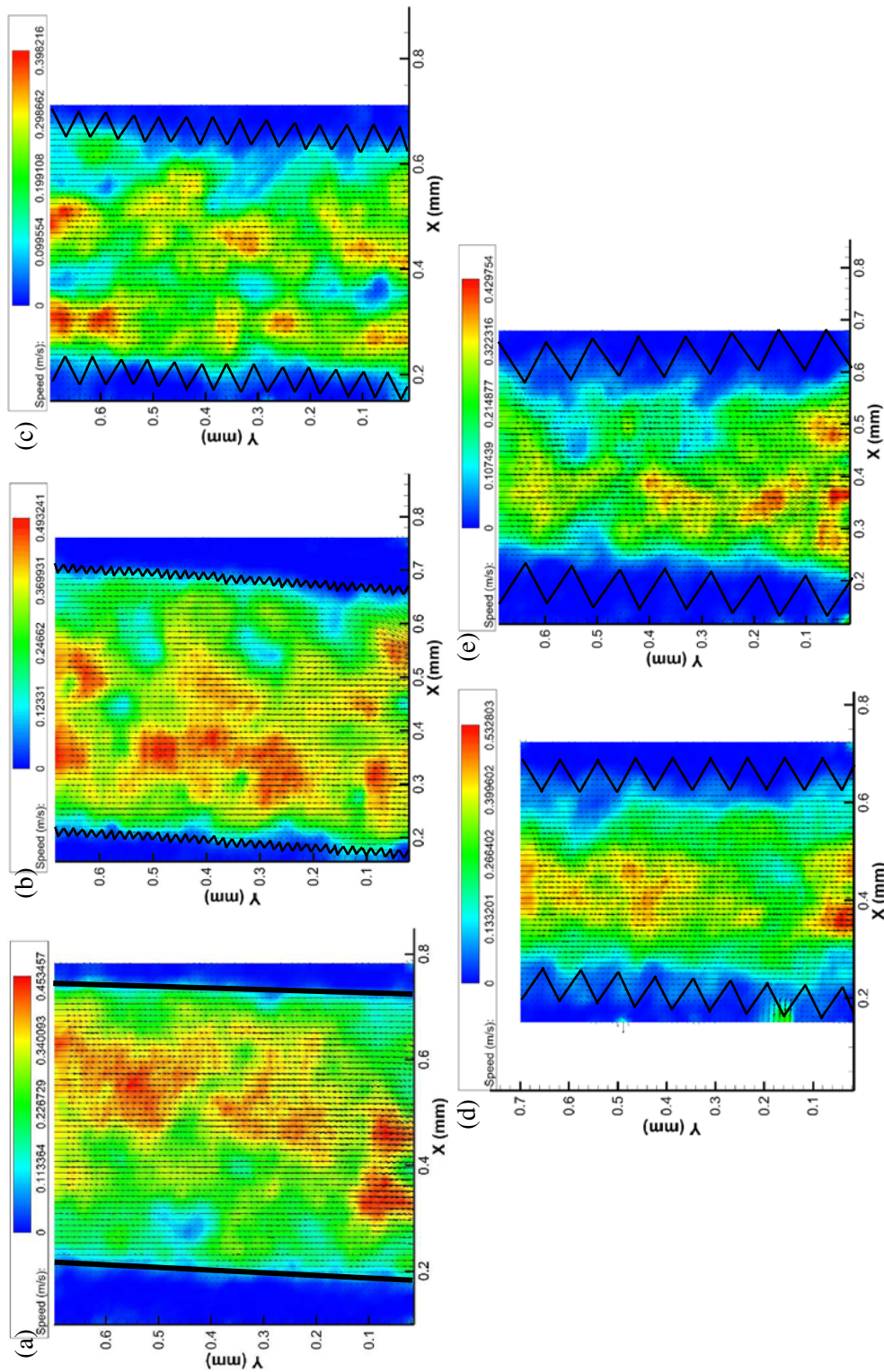


Figure 6. Velocity profile of microchannels (a) without microriblets, with microriblets size of (b) 20 μm , (c) 60 μm , (d) 80 μm , and (e) 100 μm at region 2 with the operating pressure of 200 mbar

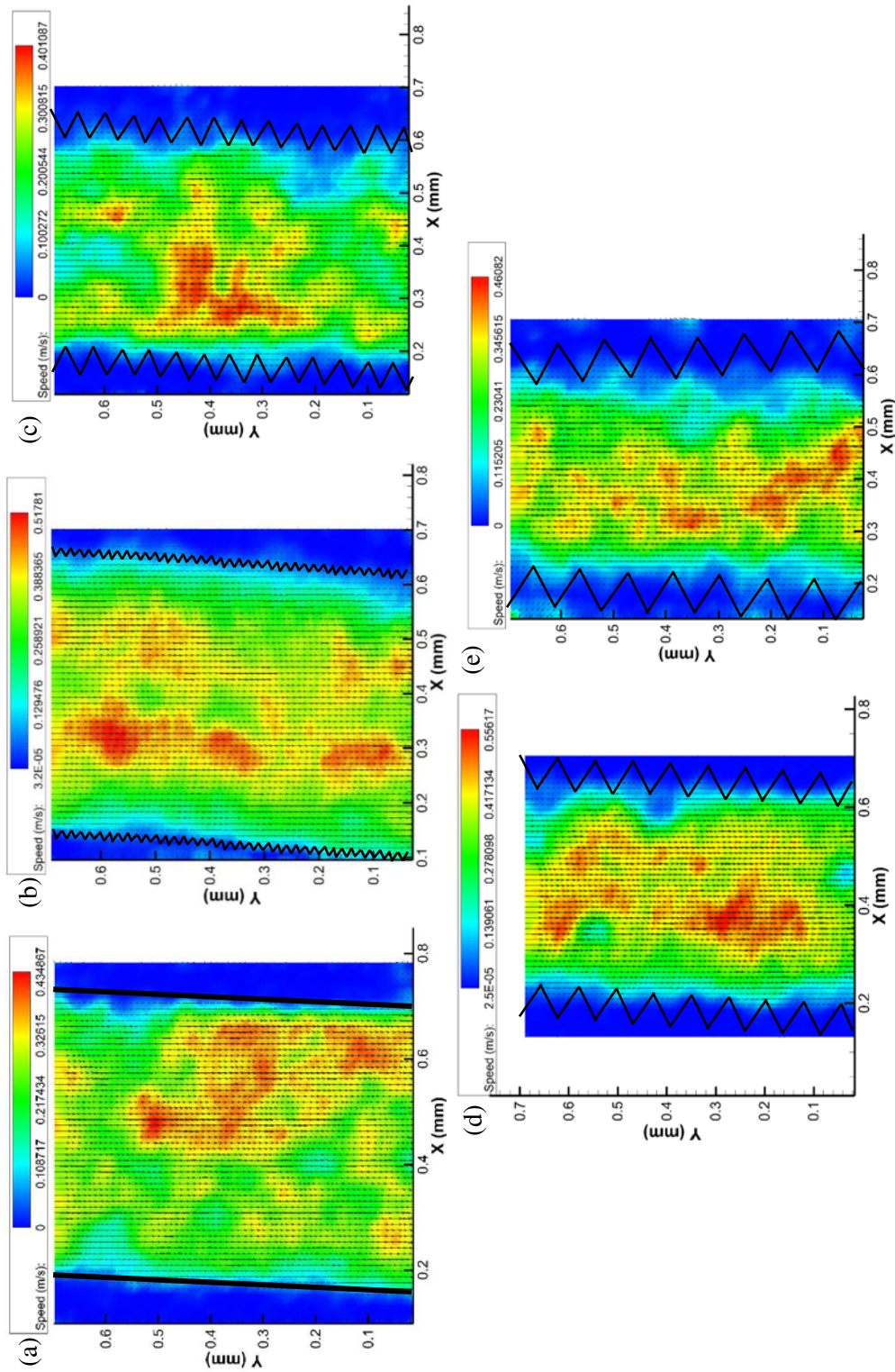


Figure 7. Velocity profile of microchannels (a) without microriblets, with microriblets size of (b) 20 μm , (c) 60 μm , (d) 80 μm , and (e) 100 μm at region 3 with the operating pressure of 200 mbar

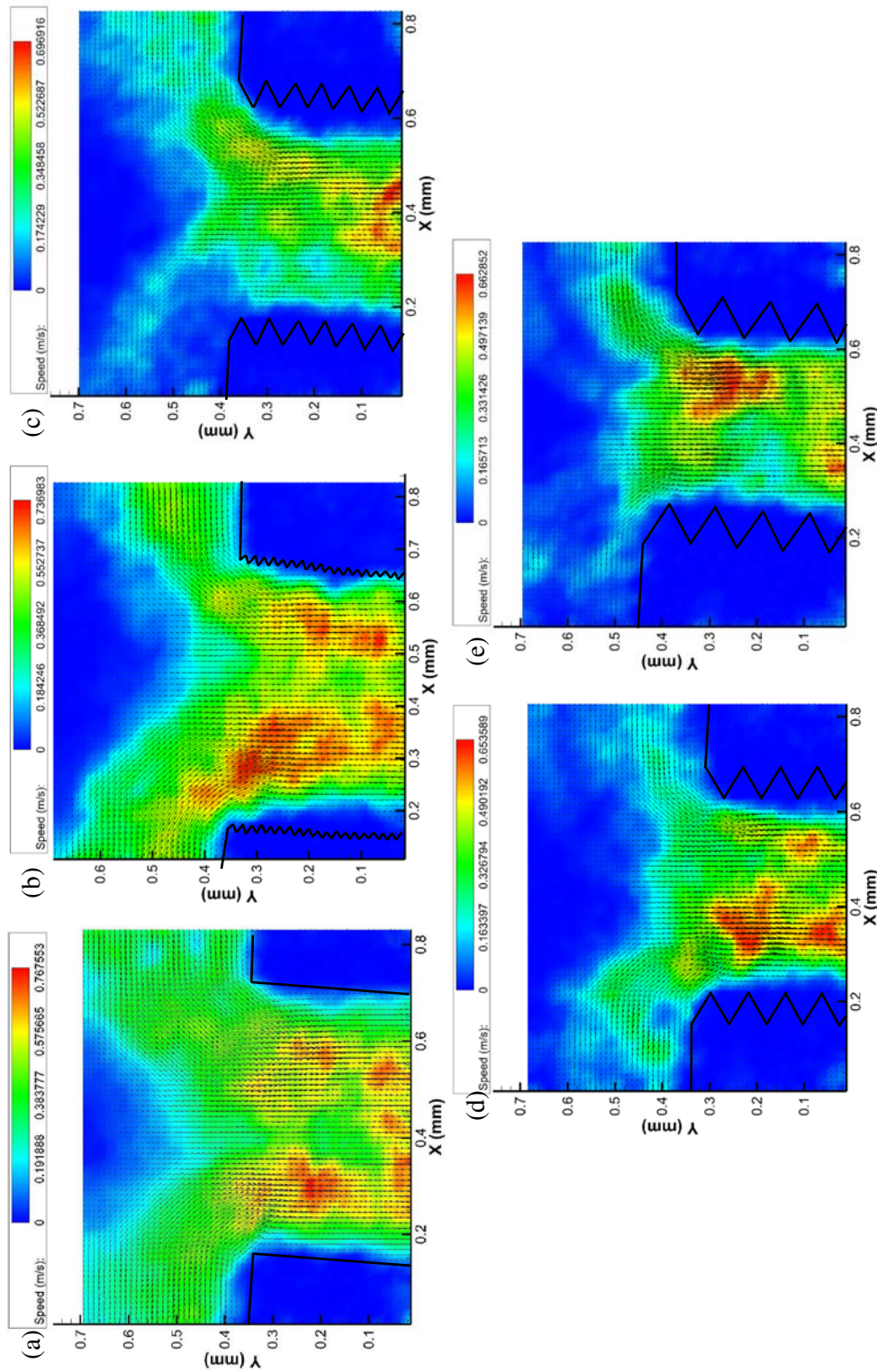


Figure 8. Velocity profile of microchannels (a) without microriblets, with microriblets size of (b) 20 μm , (c) 60 μm , (d) 80 μm , and (e) 100 μm at region I with the operating pressure of 300 mbar

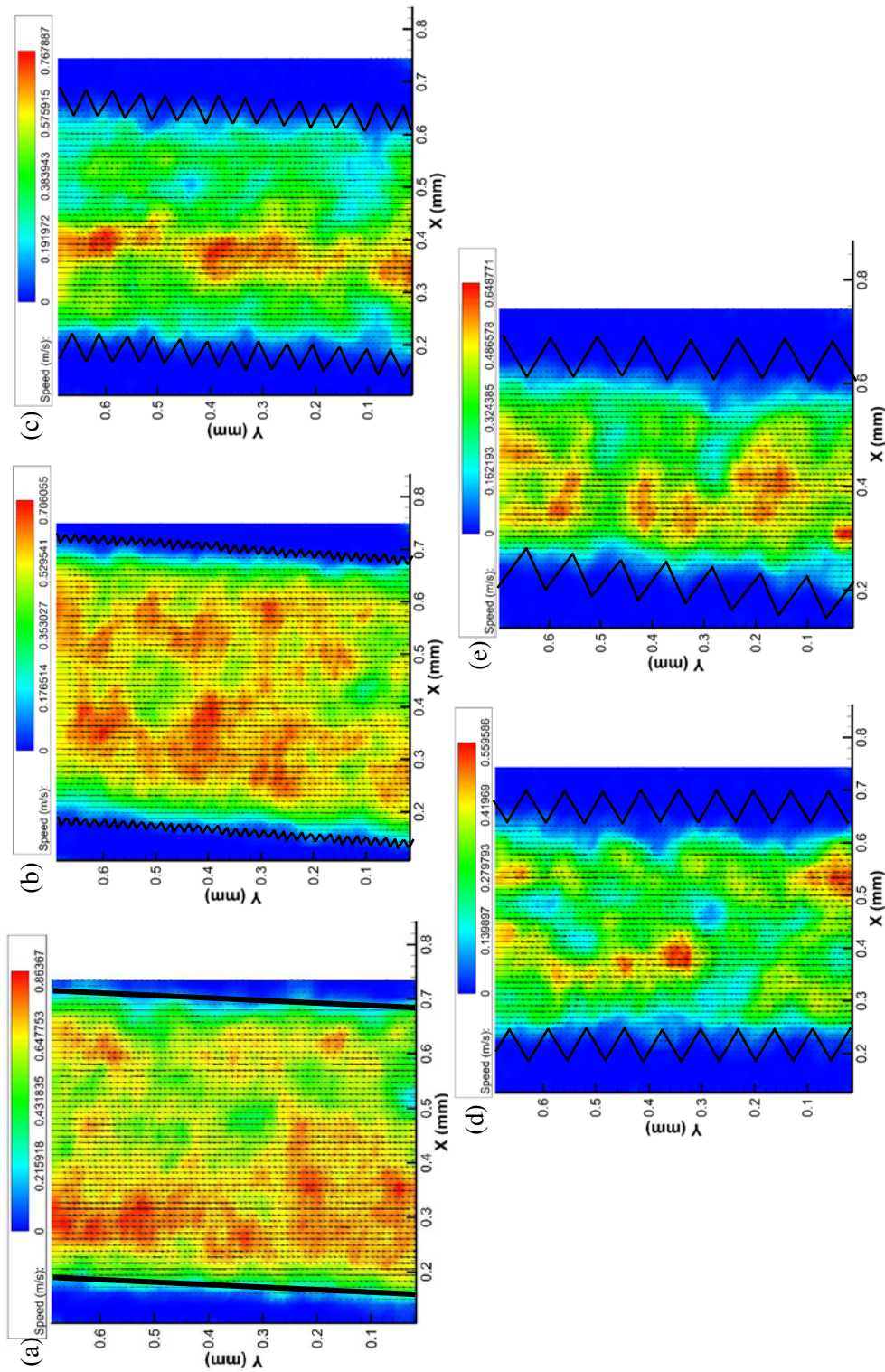


Figure 9. Velocity profile of microchannels (a) without microriblets, with microriblets size of (b) 20 μm , (c) 60 μm , (d) 80 μm , and (e) 100 μm at region 2 with the operating pressure of 300 mbar

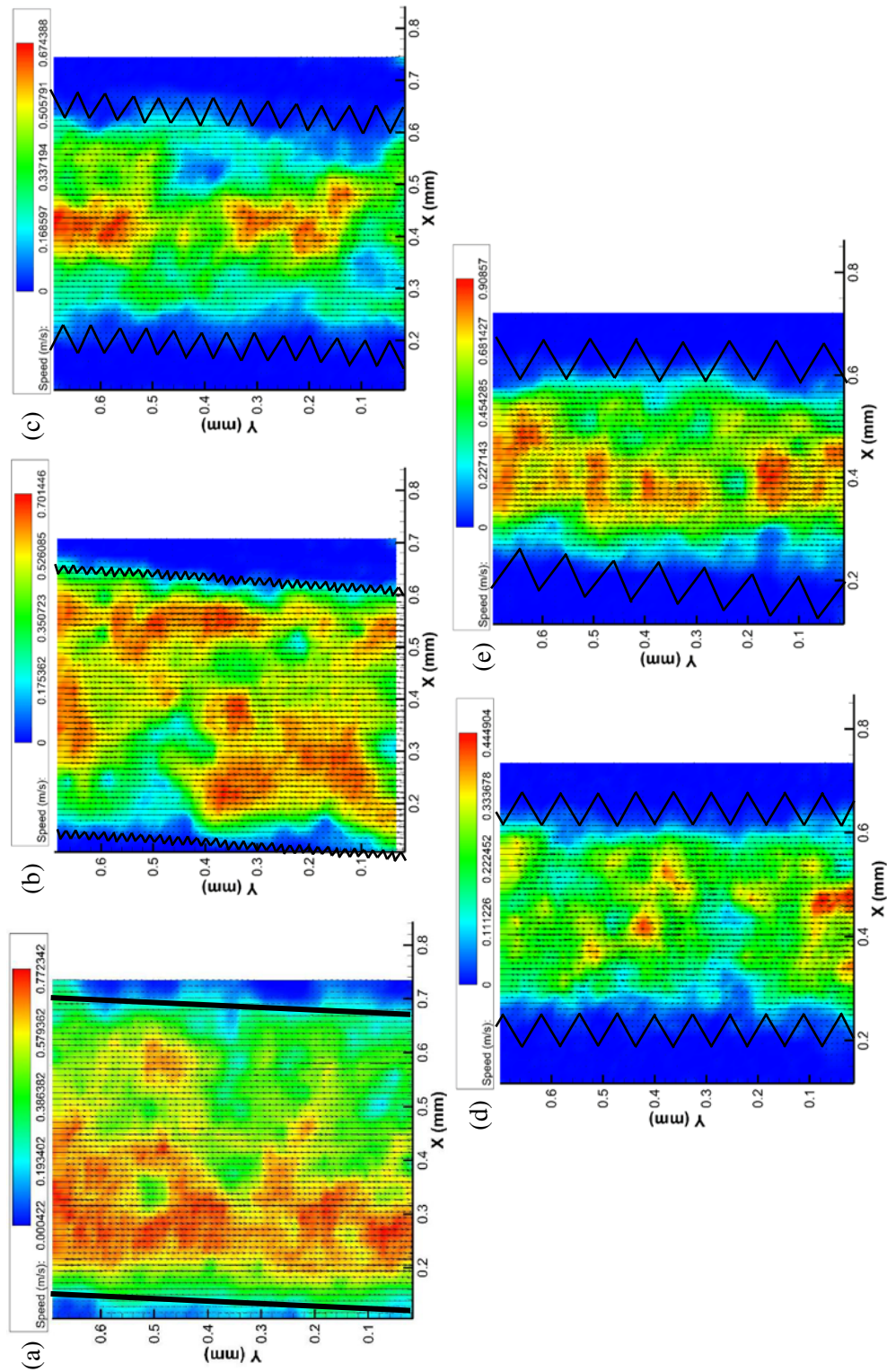


Figure 10. Velocity profile of microchannels (a) without microriblets, with microriblets size of (b) 20 μm , (c) 60 μm , (d) 80 μm , and (e) 100 μm at region 3 with the operating pressure of 300 mbar

4. Conclusions

The present work evaluated the flow behaviour in smooth and ribleted-wall T-shaped micromixers. This work succeeded in presenting an alternative design (riblets) that is structured at the narrow walls of the microchannel to investigate a possible flow enhancement and mixing efficiency. The results showed that the design is able to enhance the single liquid phase flow in the up to 28.73% within the 60 μm base-to-height ribleted microchannel at the operating pressure of 200 mbar. From μ -PIV measurements, the images clearly show that the microstructures thicken the laminar sublayer thus promote flow enhancement. It is believed that the investigated microriblets (V-shape) created stagnant liquid layers in the grooves and this layer will replace or act like the smooth wall surface but with different friction conditions. The size of the proposed riblets controls the wall friction where the balance between the mass of the trapped liquid and its apparent physical properties (viscosity and surface tension) influence the mobility of the liquid mass trapped in the groove. This will definitely result in the creation of the high speed pockets and can control the flow enhancement performances in the proposed microchannel design.

Acknowledgments

This study was supported by Malaysian Ministry of Higher Education through the fundamental research grant of FRGS/1/2016/TK02/UMP/02/1.

References

- [1] Abdulbari HA, Mohammed HD, Hassan ZBY 2015 *ChemBioEng Rev.* **2** 185
- [2] Abdulbari HA, Salleh MAM, Rashed MK, Ismail MHS 2017 *Indian J. Sci. Technol.* **10** 1
- [3] Abdulbari HA, Salleh MAM, Rashed MK, Ismail MHS 2018 *Chem. Eng. Commun.* **205** 1623
- [4] Bechert DW, Bruse M, Hage W, Vav Der Hoeven JGT, Hoppe G 1997 *J. Fluid Mech.* **338** 59
- [5] Bixler GD, Bhushan B 2013 *Adv. Funct. Mater.* **23** 4507
- [6] Dean B, Bhushan B 2010 *Philos. Trans. R. Soc. A Math. Phys. Eng. Sci.* **368** 5737
- [7] El-Samni OA, Chun HH, Yoon HS 2007 *Int. J. Eng. Sci.* **45** 436
- [8] Dean B, Bhushan B 2012 *Appl. Surf. Sci.* **258** 3936
- [9] Abu Rowin W, Hou J, Ghaemi S 2018 *Exp. Therm. Fluid Sci.* **94** 192
- [10] Eshrati M, Al-Wahaibi T, Al-Hashmi AR, Al-Wahaibi Y, Al-Ajmi A, Abubakar A 2017 *Exp. Therm. Fluid Sci.* **83** 169
- [11] Abubakar A, Al-Wahaibi T, Al-Wahaibi Y, Al-Hashmi AR, Al-Ajmi A 2014 *Chem. Eng. Res. Des.* **92** 2153
- [12] Wyatt NB, Gunther CM, Liberatore MW 2011 *J. Nonnewton Fluid Mech.* **166** 25
- [13] Abdulbari HA, Ling FWM 2017 *Chem. Eng. Commun.* **204** 1282
- [14] Ling FWM, Abdulbari HA 2017 *Indian J. Sci. Technol.* **10** 1
- [15] Mavros P, Ricard A, Xuereb C, Bertrand J 2011 *Chem. Eng. Res. Des.* **89** 94
- [16] Cai S, Higuchi Y 2014 *J. Hydrodyn. Ser. B* **26** 400
- [17] Abdulbari HA, Ling FWM 2015 *J. Eng. Res.* **12** 60
- [18] Ling FWM, Abdulbari HA, Heidarinik S 2015 *ARPJ J. Eng. Appl. Sci.* **11** 2146
- [19] Fu YF, Yuan CQ, Bai XQ 2017 *Biosurf. Biotribol.* **3** 11
- [20] Chen H, Rao F, Shang X, Zhang D, Hagiwara I 2013 *J. Bionic. Eng.* **10** 341
- [21] Kim T, Shin R, Jung M, Lee J, Park C, Kang S 2016 *Appl. Surf. Sci.* **367** 147
- [22] Barbier C, Jenner E, D'Urso B 2014 *arXiv* 1406.0787
- [23] Walsh MJ 1990 Riblets *Viscous Drag Reduction in Boundary Layers* ed D. Bushnell and J. Hefner (Washington: American Institute of Aeronautics and Astronautics) pp 203-261
- [24] Nitschke P 1984 *Experimental investigation of the turbulent flow in smooth and longitudinal grooved tubes* (National Aeronautics and Space Administration, Washington, DC.)
- [25] Choi K-S 1989 *J. Fluid Mech.* **208** 417
- [26] Khader MA, Sayma AI 2017 *IOP Conf. Ser.: Mater. Sci. Eng. (United Kingdom)* vol 232 p 012075
- [27] Li YF, Xia GD, Ma DD, Jia YT, Wang J 2016 *Int. J. Heat Mass Transf.* **98** 17

- [28] You X, Guo L 2010 *J. Hydrodyn. Ser. B* **22** 725
- [29] Ashraf MW, Tayyaba S, Afzulpurkar N 2011 *Int. J. Mol. Sci.* **12** 3648
- [30] White CM, Mungal MG 2008 *Annu. Rev. Fluid Mech.* **40** 235
- [31] Dallas V, Vassilicos JC, Hewitt GF 2010 *Phys. Rev. E – Stat. Nonlinear, Soft Matter Phys.* **82** 066303
- [32] Min T, Yoo JY, Choi H, Joseph DD 2003 *J. Fluid Mech.* 486 213
- [33] Schonfeld F, Hessel V, Hofmann C 2004 *Lab Chip* **4** 65
- [34] Dong Sung K, Seok Woo L, Tai Hun K, Seung SL 2004 *J. Micromech. Microeng.* **14** 798
- [35] Ali Asgar SB, Erik TKP, Ian P 2007 *J. Micromech. Microeng.* **17** 1017
- [36] Wang H, Iovenitti P, Harvey E, Masood S 2002 *Smart Mater. Struct.* **11** 662
- [37] Lin Y, Gerfen GJ, Rousseau DL, Yeh SR 2003 *Anal. Chem.* **75** 5381
- [38] Jiang F, Drese KS, Hardt S, Küpper M, Schönfeld F 2004 *AIChE J.* **50** 2297
- [39] Jen C-P, Wu C-Y, Lin Y-C, Wu C-Y 2003 *Lab Chip* **3** 77
- [40] Ottino JM, Wiggins S 2004 *Philos. Trans. R. Soc. A Math. Phys. Eng. Sci.* **362** 923
- [41] Lu C-S, Chen J-J, Liao J-H, Hsieh T-Y 2009 *J. Biomechatronics Eng.* **2** 13
- [42] Kelley DH, Ouellette NT 2011 *Nat. Phys.* **7** 477
- [43] Sarkar A, Narváez A, Harting J 2012 Optimization of chaotic micromixers using finite time Lyapunov exponents *High Performance Computing in Science and Engineering '11* ed Nagel WE, Kröner DB, Resch MM (Springer) p 325
- [44] Wu S-J, Hsu H-C, Feng W-J 2014 *Jpn. J. Appl. Phys.* **53** 97201
- [45] Cortes-Quiroz CA, Azarbadegan A, Zangeneh M, Goto A 2010 *Chem. Eng. J.* **160** 852
- [46] Ling FWM, Abdulbari HA 2017 *MATEC Web Conf.* **111** 1001
- [47] Viswanath PR 2002 *Prog. Aerosp. Sci.* **38** 571
- [48] Lee SJ, Jang YG 2005 *J. Fluids Struct.* **20** 659